Earthquakes and Structures, *Vol. 17, No. 5 (2019) 477-487*
DOI: https://doi.org/10.12989/eas.2019.17.5.477

Response of Skew Bridges with permutations of geometric parameters and bearings articulation

Mina F. Fakhry[a], Mostafa M. ElSayed[b] and Sameh S.F. Mehanny*

Structural Engineering Department, Cairo University, Giza, 12613, Egypt

(*Received June 19, 2019, Revised September 6, 2019, Accepted September 23, 2019*)

Abstract. Understanding the behavior of skew bridges under the action of earthquakes is quite challenging due to the combined transverse and longitudinal responses even under unidirectional hit. The main goal of this research is to assess the response of skew bridges when subjected to longitudinal and transversal earthquake loading. The effect of skew on the response considering two- and three- span bridges with skew angles varying from 0 to 60 degrees is illustrated. Various pier fixities (and hence stiffness) and cross-section shapes, as well as different abutment's bearing articulations, are also studied. Finite-element models are established for modal and seismic analyses. Around 900 models are analyzed under the action of the code design response spectrum. Vis-à-vis modal properties, the higher the skew angle, the less the fundamental period. In addition, it is found that bridges with skew angles less than 30 degrees can be treated as straight bridges for the purpose of calculating modal mass participation factors. Other monitored results are bearings' reactions at abutments, shear and torsion demand in piers, as well as deck longitudinal displacement. Unlike straight bridges, it has been typically noted that skew bridges experience non-negligible torsion and bi-directional pier base shears. In a complementary effort to assess the accuracy of the conducted response spectrum analysis, a series of time-history analyses are applied under seven actual earthquake records scaled to match the code design response spectrum and critical comparisons are performed.

Keywords: Skew Bridge; seismic effects; finite element; design response spectrum; time history; modal analysis; earthquakes

1. Introduction

Bridges, constituting a major asset in the infrastructure of any country and playing a key role in the transportation network that needs to stay somehow functioning after the occurrence of an earthquake, need to be optimally designed (e,g., Farag *et al*. 2015) in order to effectively respond to seismic hazards with minimal or contained damage. Investigation of the seismic vulnerability of bridges is hence a crucial task (e.g., Liu *et al*. 2017, Ghosh and Padgett 2012). Skew bridges, despite showing some inherent deficiencies from a structural perspective, are sometimes the solution for crossing non-orthogonal roads that are frequently encountered due to some planning/alignment constraints. Comprehensive modeling of such special bridges under general earthquake loading conditions aiming at identifying their seismic response and highlighting their pros and cons and/or vulnerability to seismic hazards has been conducted by many researchers (e.g., Kun *et al*. 2018, Chen and Chen 2016, Ramanathan *et al*. 2015, Ayoub *et al*. 2013, 2014, Apirakvorapinit *et al*. 2012, Whelan and Janoyan 2012, Apirakvorapinit 2005, Maleki 2001, 2002, 2005, Meng and Lui 2000, Wakefield *et al*. 1991). The present research is a further step along this road targeting a better understanding of the seismic response of skew bridges with various support conditions, skew angles, skew aspect ratios (width/span), etc. The analytical results presented herein include modal characteristics, as well as support reactions, pier internal forces, and deck deformations under the action of selected and scaled actual earthquake records, in addition to a traditional codified response spectrum analysis for design purposes considering code design response spectrum.

2. Modal properties of archetypical Skew Bridges

2.1 Description and modelling of the archetypical case-study bridges

Different versions of skew bridges are designed to fulfill relevant code requirements for seismic design (ECP 201 2008). Key dimensions and characteristics are shown in Fig. 1, where W, L, H, and β are bridge's width, span-length, pier height, and skew angle, respectively. Bridge's deck and piers are modeled using 2D shell and 1D frame elements, respectively (CSI-SAP2000 software). Linear concrete constitutive model, with Young's modulus "E" and Poisson's Ratio "ν" equal 24 000 MPa and 0.2, respectively, are used in modeling both previously mentioned shell and frame elements.

*Corresponding author, Professor
E-mail: sameh.mehanny@stanfordalumni.org
[a]Graduate Student
E-mail: minafayez487@gmail.com
[b]Assistant Professor
E-mail: elsayemm@gmail.com

http://www.techno-press.com/journals/eas&subpage=7
ISSN: 2092-7614 (Print), 2092-7622 (Online)

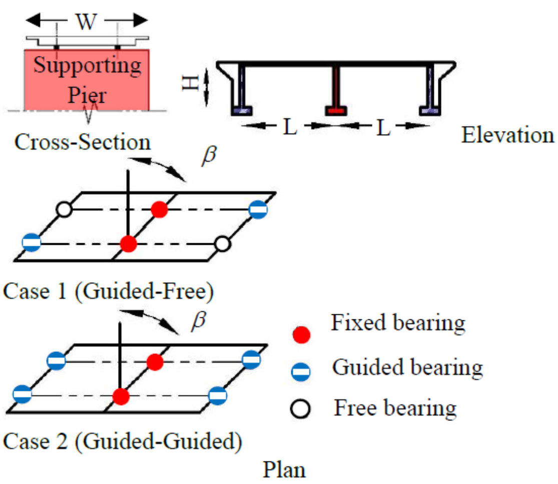

Fig. 1 Geometric characteristics of the case-study bridge

In this paper, seven different skew angles varying from zero to 60 degrees are considered with a 10-degree increment. Skew angle is simulated in the FE model through rotating local axes of the pier (and bearings) frame elements, and subsequently deck shells. Moreover, two cases of bearing articulations at abutments (namely, guided and free) are investigated in this study. To simulate guided condition, only the degree of freedom along the longitudinal axis of the bridge is allowed, while in case of free bearing articulations both longitudinal and transversal degrees of freedom are allowed. In addition, two pier fixities (viz. monolithic piers and piers with fixed bearings) are considered at the pier top junction with the deck, while fixed supports are utilized to simulate the foundation. In case of piers with fixed bearings atop, a moment release is introduced at the top of the frame elements representing the bearings (see Fig. 2). In addition, rigid links are used to connect the top node of the frame element modeling the pier, and located along its axis, to the soffit of the vertical frame elements modeling the bearings (Ayoub *et al*. 2014), as also shown in Fig. 2.

Three cases of span configuration (two and three spans 20 m each, and another model with two spans 30 m each), two deck widths (10 m and 14 m), two different pier heights (7 m and 14 m), and two pier cross sections (circular and rectangular with its transverse dimension equal to the deck width) are considered. The total number of bridges studied in this manuscript is more than 900 bridges. Furthermore, seismic masses are calculated to account for the total dead and superimposed dead loads and the applicable percentage (namely 20%) of the live loads as per code (ECP 201 (2008)), and are then distributed among deck shells. Finally, cracked sections are assigned to reinforced concrete piers when both modal and time history analyses are performed.

2.2 Skew angle and modal properties

Modal analysis is a vital step to understand the response of skew bridges under earthquake (dynamic) loads. In this study, two parameters (periods of vibration and modal mass participation) are utilized to judge the influence of changing skew angle on the modal properties of the case study bridges considering various design parameters, as shown in Fig. 3.

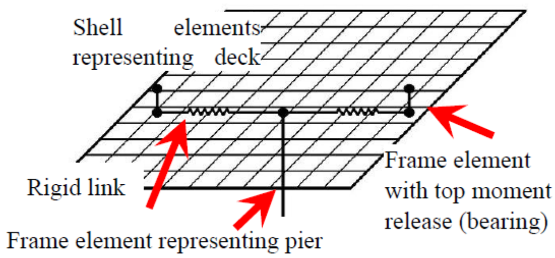

Fig. 2 Finite-element details for the pier-to-deck connection of the skew bridge shown on a part-model (case of pier with fixed bearings)

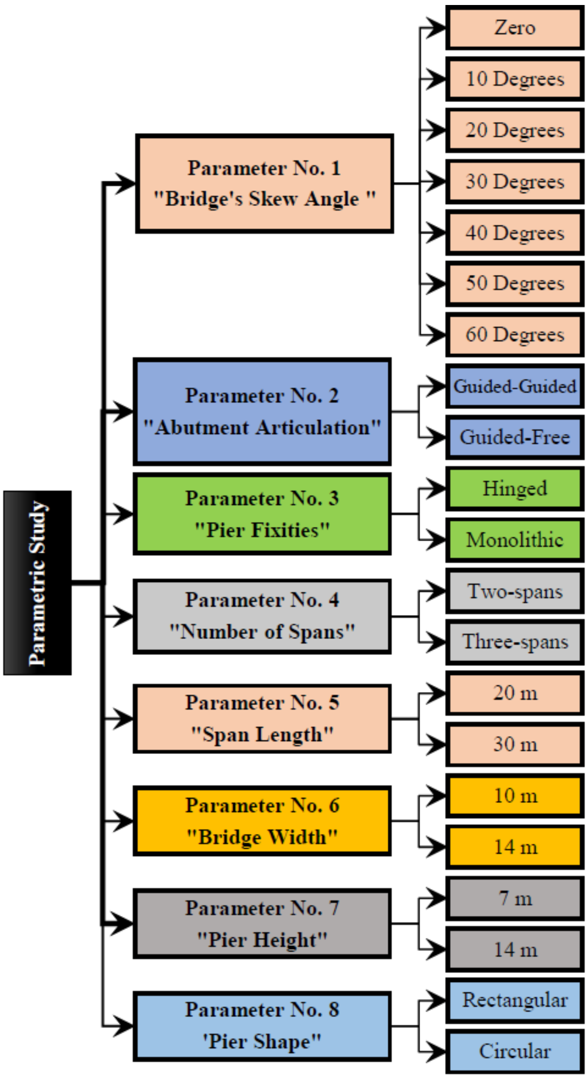

Fig. 3 Various investigated parameters for the case-study skew bridges

By analysing the period of vibration results, it has been observed that a higher skew angle reduces the fundamental period of the bridge, while the remaining periods of other modes of vibration are almost unaltered (see figure 4). The average reduction in the fundamental period considering rectangular and circular pier shapes (per a 10-degree change in skew angle) is around 20 % and 5 %, respectively. In addition, using 7.0 m pier height instead of 14.0 m leads to an around 36% reduction in the fundamental period.

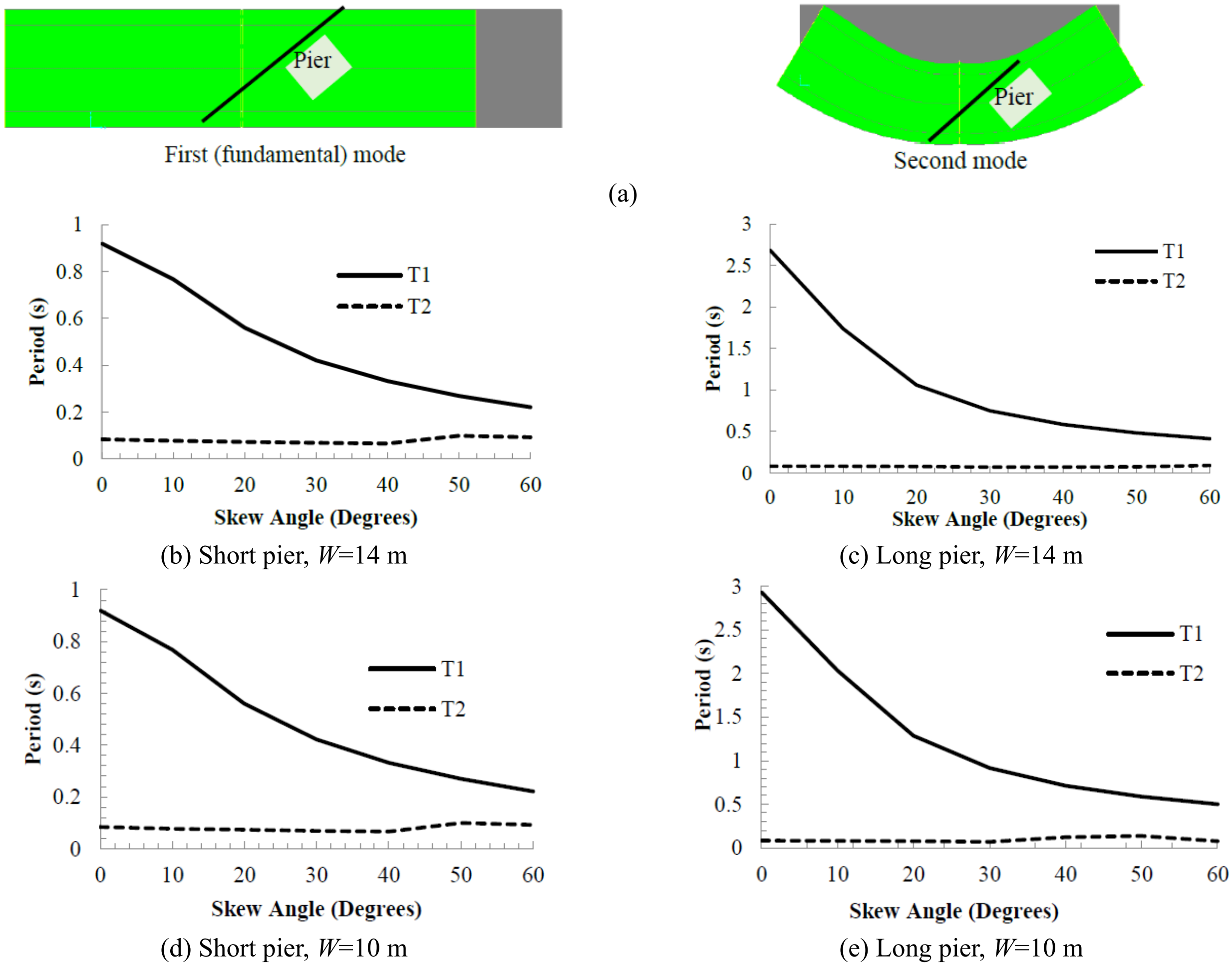

Fig. 4 (a) First and second mode shapes in plan, and (b)-(e) influence of the skew angle on the two-span (20-20 m) bridges' periods considering short and long piers for two different bridge widths (W=10 and 14 m)

Moreover, using monolithic piers (fully fixed for rotation and translation) instead of hinged piers (only restraining translation degrees of freedom) results in a reduction around 34 % in the fundamental period. Finally, parameters 2, 4, 5, and 6 identified in Fig. 3 have a negligible influence on the fundamental period.

For skew angles less than 40 degrees, the summation of both longitudinal modal mass participation factors (M_{ux}) and transverse modal mass participation factors (M_{uy}) of the first mode is almost 100%. This is due to the virtual absence of torsion effects. In general, the higher the skew angle, the lower the M_{ux} and the higher the M_{uy} of the first mode. However, variation in these two factors is negligible for skew angles less than 50 degrees, as illustrated in Fig. 5. On the other hand, the higher the skew angle, the higher the M_{ux} and the lower the M_{uy} of the second mode.

It is nonetheless worth noting that using circular piers leads to almost constant modal mass participation factors as follows:

- M_{ux} of the first mode is higher than 99%
- M_{uy} of the first mode is less than 1 %
- M_{ux} of the second mode is less than 1%
- M_{uy} of the second mode is higher than 75%

For rectangular piers, on the other hand, only abutment bearings' articulation and pier height have significant effects on the modal mass participation factors, while the remaining studied parameters as identified in Fig. 3 have negligible effect:

- Studying the second parameter in Fig. 3 (namely, abutments bearing articulations) shows variations in both M_{ux} and M_{uy} of the first and second modes of vibration up to 35%, 50%, 40% and 25%, respectively.
- However, studying the third parameter (pier fixities, i.e., hinged versus monolithic piers) shows average variations in both M_{ux} and M_{uy} of the first and second modes up to 3.40%, 0.75%, 0.82% and 1.36%, respectively.
- Considering two and three-span configurations shows an insignificant influence on the variation in mass participation factors (less than 6%).
- In addition, changing span length leads to an average variation of 10% for M_{ux} of the first mode and 5% for the remaining mass modal participation factors.
- Moreover, changing bridge width shows an insignificant influence on the variation in mass participation factors (less than 6%).

3. Response of Skew Bridges

3.1 Code design response spectrum

As previously mentioned, about 900 finite-element

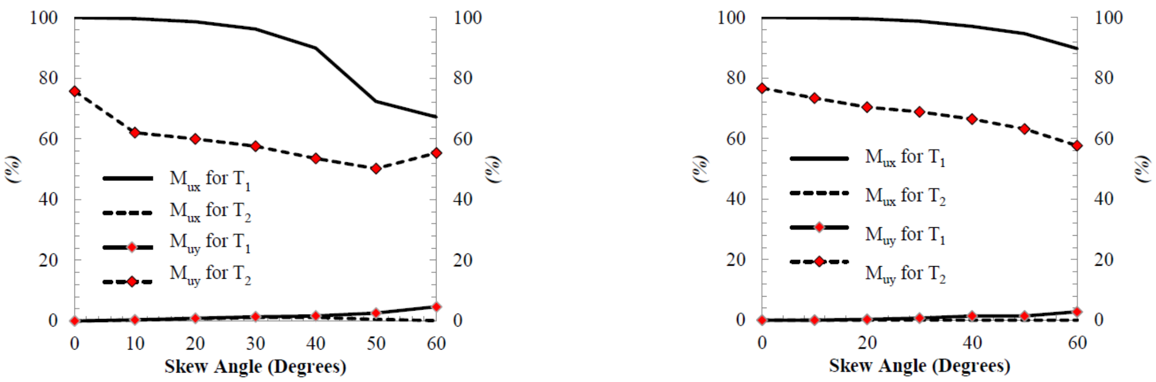

(a) Short pier with guided-guided bearings on abutment (b) Long pier with guided-guided bearings on abutment

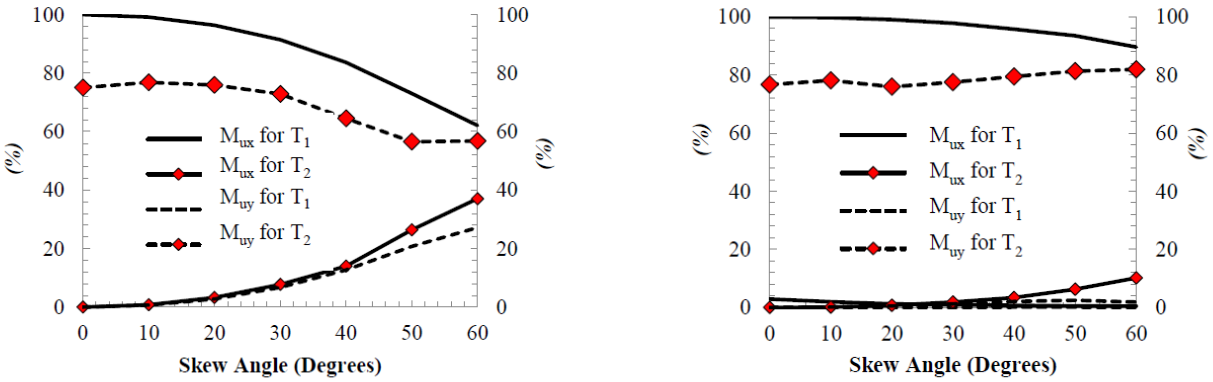

(c) Short pier with guided-free bearings on abutment (d) Long pier with guided-free bearings on abutment

Fig. 5 Influence of skew angle on the mass participation coefficient for the two-span (20-20 m) with 10m width bridges considering short and long piers, for two different bridge bearings articulations

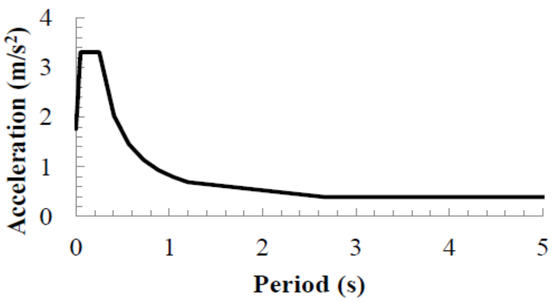

Fig. 6 Design response spectrum (DRS) as per ECP 201 (2008)

models are analysed using ECP 201 (2008) design response spectrum (DRS) in order to determine case-study bridges' straining actions and deformations for seismic design purposes. The DRS shown in Fig. 6 is as per ECP 201 (2008) Type 1 response spectrum, and is constructed for a reference peak ground acceleration of 0.1 g, soil type A, a bridge importance factor of 1.3, and an elastic behaviour (i.e., for a response modification/behaviour factor of 1.0 in order to neutralize its effect on the seismic response of all investigated bridge configurations). The DRS as per ECP 201 (2008) features a code-imposed constant minimum design acceleration as shown effective in Fig. 6 for long periods in order to enforce some conservatism in design. The following sections illustrate the influence of skew angle on pier base shear, torsion, bearing reaction and deformations under the action of both longitudinal and transverse earthquake load cases.

3.2 Pier base shear, V_{22}

Fig. 7 illustrates the different monitored trends between pier base shear, V_{22}, and skew angle when the earthquake load is applied in the bridge's longitudinal direction. V_{22} is the shear along an axis with a clockwise angle β (i.e., the skew angle) measured from the bridge longitudinal axis. It also represents the pier weak-axis base shear for the bridge configuration with rectangular piers. In general, three trends are observed, and are accordingly categorized in three cases as follows with the average result values for each category reported in Fig. 7. The first category, referred to as Cat. A1 in Fig. 7, represents - for each investigated skew angle - bridges with two spans (20 m span-length and 10 m deck width), resting on 7.0 m circular piers. The total number of the bridges of this group is 4 out of 128 bridges (3.1%). The second category, Cat. A2, represents for each studied skew angle bridges resting on 14.0 m circular piers, which are 32 out of 128 bridges (25%). Finally, the third category, Cat. A3, represents the remaining tested bridges, which are the majority and equals 92 cases out of 128 (71.9%). It is to be noted that the 128 bridges mentioned herein are the various bridge configurations encompassing all permutations of the investigated parameters 2 through 8 identified in Fig. 3 for each studied skew angle. Hence, for all the six considered skew angles - as per parameter 1 in Fig. 3 - in addition to the case of the straight bridge (i.e., the zero-skew bridge scheme), the total number of investigated bridge configurations is 896 (i.e., 128×7

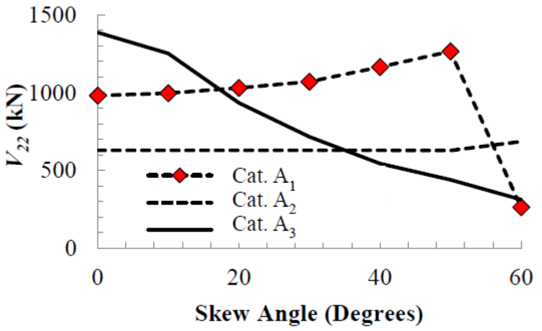

Fig. 7 Relationship between pier base shear, V_{22}, and skew angle under longitudinal earthquake load case (results reported in figure are the average values for each category)

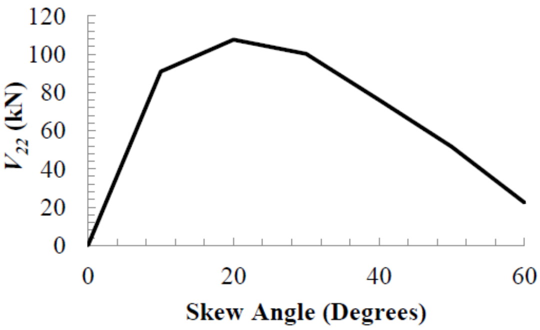

Fig. 8 Relationship between pier base shear, V_{22}, and skew angle when transverse earthquake is applied

viz. about 900).

Referring to Fig. 7, for Cat. A1, V_{22} slightly increases as skew angle increases till a sudden drop for angles higher than 50 degrees. Similar to previous case, V_{22} in Cat. A2 is slightly increased as skew angle increases, but no sudden drop is observed. Nevertheless, on the other hand, the higher the skew angle, the less V_{22} in Cat. A3.

Other specific observations vis-à-vis pier strong axis base shear when the earthquake is applied in the bridge's longitudinal direction are as follows - for supporting details the reader is referred to Fakhry (2019):

• The effect of abutment articulation is negligible.

• Using hinged piers instead of monolithic ones leads to reduced V_{22} values by 30 % for straight bridges, and the reduction ratio increases as the skew angle increases. For example, the V_{22} values of hinged piers is less than the corresponding values - but with monolithic piers - by 75% for the skew angle of 60 degrees. This observation is not valid for bridges resting on 14.0 m-high circular piers.

• In addition, considering three-span configuration instead of the two-span one leads to a reduction in V_{22} by an average 20% for non-skewed (i.e., straight) bridges, while it reduces to be around 8% for 60 degrees skew angle which means that the skew effect on V_{22} is reduced for greater number of spans.

• On the other hand, increasing span-length by 50 % leads to an increase in V_{22} by an average 20% for straight bridges. The reduction in V_{22} ratio reduces to be 8% for 60 degrees skew angle which means that the effect of skewness on V_{22} is reduced for longer span-length.

• Moreover, considering 14 m deck width instead of 10 m develops higher V_{22} values. The increase ratio is around 20 % for zero skew bridges, while it reduces to be only around 6% for 60 degrees skew angle which means that the skew effect on V_{22} is reduced for wider decks.

• The higher the pier, the less the base shear. In addition, skew angle effect on V_{22} is reduced for higher piers. Namely, the average reduction ratio in V_{22} is around 45% for zero skew bridges, while it reduces to be only around 25% for 60 degrees skew angle bridges.

• Finally, straight bridges with rectangular piers have greater V_{22} values than corresponding values with circular ones by around 35%. On the other hand, V_{22} remains almost the same (up to a skew angle of 50 degrees) for circular piers while it reduces significantly for rectangular piers. As such, pier shape has an important influence on the V_{22} values.

Fig. 8 illustrates the relationship between V_{22} values and skew angle when earthquake is applied in the bridge's transverse direction. In general, the developed V_{22} values are significantly less (around 90% reduction) compared to the corresponding base shear values when earthquake is applied in the longitudinal direction of studied bridges. This is due to the significant difference in bridge's periods corresponding to both longitudinal and transversal directions. It is worth mentioning that the average peak V_{22} values are less than 120 kN, except for bridges with short piers and guided-free abutment articulations. However, unlike straight bridges, V_{22} cannot be neglected when earthquake is applied in the transversal direction of skew bridges.

In general, there is a sudden increase in V_{22} values and the peak value occurs at a skew angle of about 20 degrees (see Fig. 8). Similar to modal properties, using monolithic pier fixation, increasing number of spans and increasing span-length, and using rectangular piers instead of circular ones significantly influence base shear values up to three folds. In addition, reducing pier height to half results in around ten times the V_{22} values. On the other hand, changing bridge width has an insignificant effect on base shear values.

3.3 Pier base shear, V_{33}

In general, three trends for the relationship between pier base shear, V_{33}, and skew angle are observed when earthquake is applied in the longitudinal direction of the case study bridges (see Fig. 9). V_{33} is the shear along an axis with an anti-clockwise angle 90^o-β measured from the bridge longitudinal axis. It also represents the pier strong-axis base shear for the bridge configuration with rectangular piers. In general, straight bridges always experience zero values of V_{33} under longitudinal earthquakes that then increases as the skew angle increases. The first category of bridges, referred to as Cat. B1, represents the two-span configuration (20 m span-length and 10 m deck width), resting on 7.0 m circular piers. The total number of bridges of this category is 4 out of the 128 bridges (3.1%) marking all permutations of investigated parameters 2 through 8 identified in Fig. 3 for each considered skew angle. The second category, Cat. B2, represents similar bridges to those of the previous

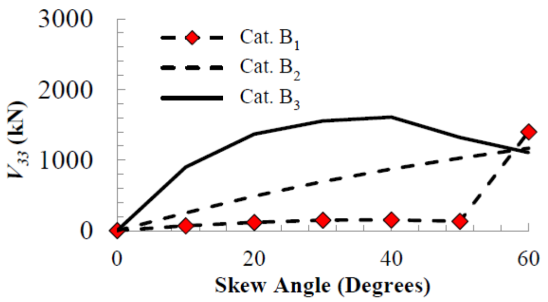

Fig. 9 Relationship between pier base shear, V_{33}, and skew angle when longitudinal earthquake is applied (results reported in figure are the average values for each category)

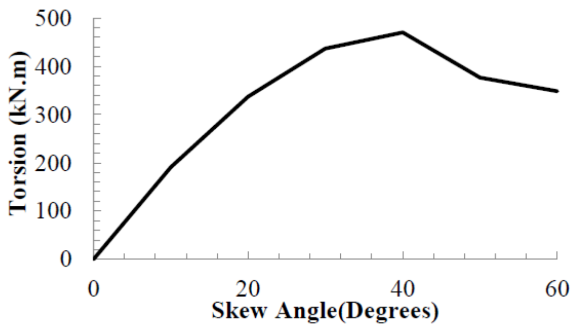

Fig. 10 Relationship between torsion and skew angle when longitudinal earthquake is applied

group, but featuring three spans instead of two spans. Therefore, the total number of bridge configurations in this category is also 4 out of 128 bridge permutations (3.1%). Finally, the third category, namely Cat. B3, represents for each investigated skew angle the remaining 120 bridges, which are the majority (93.8%). Unlike straight bridges, V_{33} cannot be neglected when earthquake is applied in the longitudinal direction of skew bridges.

A few specific observations regarding the pier base shear, V_{33}, when the earthquake is applied in the bridge's longitudinal direction are as follows - the reader is referred to Fakhry (2019) due to space limitations:

• The effect of abutment articulation is negligible.

• In general, using hinged or monolithic piers does not affect the values of V_{33}. This is valid for all cases except where long and circular piers are used, in which ten-times the shear is expected when hinged piers are used instead of monolithic ones.

• Similar to V_{22}, considering three-span instead of two-span configurations leads to a reduction in V_{33} by an average of 25% for 60 degrees skew angle bridges, which means that the effect of skewness on V_{33} is increased for greater number of spans.

• The influence of span-length on V_{33} is negligible.

• Considering 14 m deck width instead of 10 m develops higher V_{33} values but this is simply mainly due to the increase in the seismic mass. An increase ratio could be calculated between the pier base shear of 14 m width bridges to the corresponding shear values in 10 m width bridges. This ratio is around 50% for 60 degrees skew bridges, while it reduces to be around zero for straight bridges which means that skew angle effect on V_{33} is increased for wider decks.

• Moreover, considering 14 m pier height instead of 7 m develops lower V_{33} values. The reduction ratio in base shear values is around 60% for 60 degrees skew angle bridges, and gets smaller as the skew angle reduces which means that skew effect on V_{33} is increased for case study bridges with higher piers.

• Finally, when considering rectangular piers instead of circular ones, higher V_{33} values are developed. In addition, the higher the skew angle, the more the variation in V_{33} that may reach 80% for 60 degrees skew angles.

On the other hand, straight bridges experience a non-negligible pier base shear, V_{33}, when the earthquake is applied in the bridge's transverse direction.

3.4 Effect of investigated parameters on Pier's torsion

Whether the earthquake is applied in bridge's longitudinal or transverse direction, torsion effect on piers is only observed in three-span skew bridges, while it can be practically neglected in skew two-span bridge configurations considered herein. When earthquake is applied in the bridge's longitudinal direction, torsion induced in piers is directly proportional to the skew angle till it reaches its peak value at a skew angle around 40 degrees, then it reduces by 25% for a skew angle of 60 degrees (see Fig. 10). Specific observations when the earthquake is applied in the three-span bridge's longitudinal direction are as follows:

• The most significant parameter is the pier shape; using rectangular piers leads to higher torsion than utilizing circular piers by about 15 times.

• The second affecting parameter is the pier height; using 7 m-high piers leads to almost double the induced torsion of the 14 m-high piers.

• Rest of tested parameters of Fig. 3 have an insignificant effect on torsion in the piers of the case study skew bridges.

On the other hand, the relationship between torsion induced in piers and skew angle cannot be predicted, as it simultaneously depends on all tested parameters previously detailed in Fig. 3.

3.5 Effect of investigated parameters on abutment bearings transverse reactions

Fig. 11 illustrates the relationship between a predefined ratio, R_a, of the transverse reaction of the abutment's longitudinally guided bearings and the skew angle when the earthquake is applied in the longitudinal direction. R_a is identified as the ratio between the peak abutment bearing's transverse reaction and the bridge's seismic weight, the latter being simply the bearing's vertical reaction from seismic weight. Unlike straight bridges, skew bridges with longitudinally guided bearings at abutments experience non-zero values for R_a under longitudinal earthquakes. The first category in Fig. 11, referred to as Cat. C1, represents for each investigated skew angle all permutations of the case study bridges with guided-guided abutment articulation and rectangular pier's shape (25% of investigated models), while the second category, namely Cat. C2, represents the remaining studied bridges for each specific skew angle, i.e.,

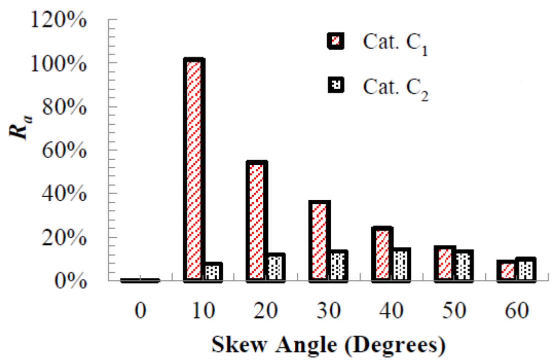

Fig. 11 Relationship between R_a and skew angle when longitudinal earthquake is applied (results reported in figure are the average values for each category)

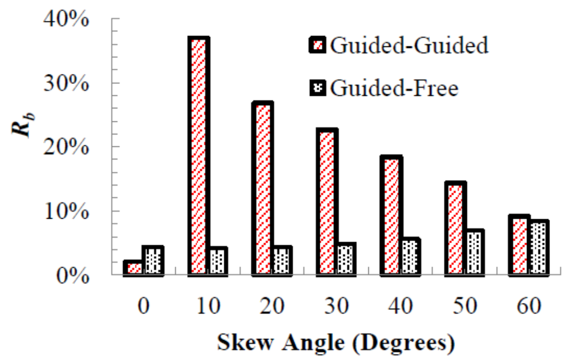

Fig. 12 Relationship between R_b and skew angle when transverse earthquake is applied

those with guided-free bearings. In Cat. C1, R_a marks a peak value at a skew angle of 10 degrees. Afterwards, a reduction in R_a is observed as the skew angle increases, where it reaches a value of only 10% for 60 degrees skew angle. The large increase in the transverse reaction of guided-guided bearings atop of abutments at small skew angles (namely up to 20 degrees) is mainly due to the significant in-plane seismic moment arising from the longitudinal earthquake hit that is then translated into a force-couple carried by the two guided bearings closely distant due to the relatively small skew angle. On the other hand, a directly proportional - but with a very mild change - relationship is noted between R_a and the skew angle for Cat. C2 of bridges featuring guided-free bearings atop of abutments; R_a is typically less than 10% and thus, it can be neglected. Note that for guided-free bearings configuration, there is no in-plane seismic moment, and hence no force-couple, generated at the abutment since the transverse reaction is only carried by one single bearing atop of each abutment, namely the guided bearing. It is worth stating that the current investigation is performed for discrete skew angles ranging from zero (i.e., case of straight bridge) to 60 degrees with a 10-degree increment.

Considering only the more influential category of bridges (namely Cat. C1 in Fig. 11), the following observations may be drawn - for more details and supporting data the reader is referred to Fakhry (2019):

- In general, using monolithic instead of hinged piers reduces the peak values of R_a by about 25%.
- In addition, considering three-span instead of two-span configurations leads to an increase in peak R_a values by an average of 18% for the 14 m-high pier bridges. On the other hand, a reduction in peak R_a by an average of 22% is observed for 7 m-high pier bridges for the three-span configuration.
- Furthermore, increasing the span-length by 50% leads to a decrease in the peak R_a value by an average of 35%.
- Moreover, increasing bridge width by 40% leads to a reduction in the peak R_a value by an average of 23%.
- Finally, increasing pier height leads to a slight decrease in the peak R_a value by an average less than 15%.

On the other hand, the relationship between abutment bearing's transverse reaction ratio, R_b, and the skew angle is illustrated in Fig. 12 when the earthquake is applied in the transverse direction of the bridge. R_b is defined as the ratio between the abutment bearing's peak transverse reaction due to transverse earthquake and the bearing's vertical reaction from seismic weight. For bridges with guided-guided abutment articulation, R_b-similar to R_a-reaches a peak (about 40%) at the small skew angle of 10 degrees. Afterwards, a reduction in R_b is observed as the skew angle increases, which may reach 10% for 60 degrees skew angle. On the other hand, the effect of the skewness on R_b for guided-free abutment articulations is negligible.

Specific observations when earthquake is applied in the bridge's transverse direction are as follows:

- The effect of pier fixity on R_b is negligible.
- Increasing number of spans leads to an increase in the value of R_b for guided-guided abutments, and a reduction for guided-free abutments. For example, considering the three-span configuration instead of the two-span bridges leads to an increase of 25% and a reduction of 38% for guided-guided and guided-free abutment articulations, respectively.
- The more the span length, the greater the value of R_b for guided-guided abutments, and the less the value of R_b for guided-free abutments. For instance, increasing span length by 50% leads to an increase in R_b by 30% and a reduction by 47% for guided-guided and guided-free abutment articulations, respectively.
- The wider the bridge, the less the value of R_b. For example, considering the 14 m-wide bridge instead of the 10 m-wide bridge leads to a reduction in R_b by around 20%.
- Last but not least, increasing pier height (from 7 m to 14 m) leads to an increase in R_b by around 60% and 5% for rectangular and circular piers, respectively.

3.6 Effect of various investigated parameters on Deck's displacement

In this section, the longitudinal displacement of the bridge deck, Δ_x, is studied when the earthquake is applied in the longitudinal direction. Fig. 13 illustrates the different trends of the relationship between longitudinal deck displacement, Δ_x, and the skew angle when the earthquake is applied in the bridge's longitudinal direction. In general, two trends are observed and are categorized as follows. First category, referred to as Cat. D1, represents for each studied skew angle all permutations of bridges resting on circular piers

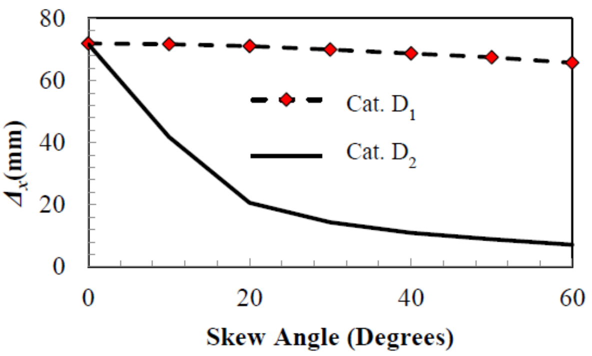

Fig. 13 Relationship between longitudinal deck displacement and skew angle (results reported in figure are the average values for each category)

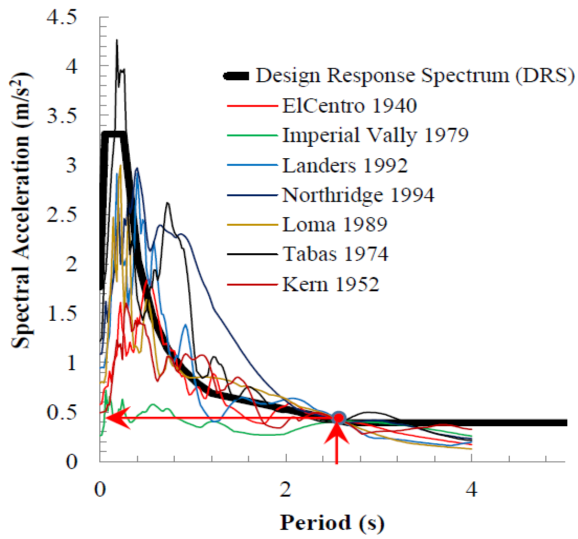

Fig. 14 Sample scaling of the selected seven actual earthquake records to the code DRS at the fundamental period of one case study skew bridge. (The dot in the figure is the scaling point for the shown sample case)

with monolithic connection. The total number of bridges in this group is 32 out of 128 bridges (i.e., the quarter). The second category, namely Cat. D2, represents, again for each skew angle, the remaining permutations of investigated bridges which constitutes the majority (96 cases out of 128 bridges, i.e., 75%). In the first category, Cat. D1, the effect of the skew angle on Δ_x is almost negligible. On the other hand, Δ_x for Cat. D2 is inversely proportional to the skew angle with a steep relation for small skew angles (up to 20 degrees) followed by a mild relation for larger skew angles up to the largest studied (namely, 60 degrees).

Specific observations when the earthquake is applied in the bridge's longitudinal direction are as follows:

- The effect of the abutment articulation is negligible.
- Using hinged piers instead of monolithic ones leads to an increase in Δ_x by an average of 45% for straight bridges. On the other hand, the higher the skew angle, the less the influence of pier fixity on deck's displacement with a 5% difference for a skew angle of 60 degrees.
- In addition, considering the three-span configuration instead of the two-span bridges leads to an increase in Δ_x by an average of 17% for non-skewed bridges. Similar to previous observation, the higher the skew angle, the less the influence of number of spans on longitudinal deck displacement with a minimum difference of 13% for 60 degrees skew angle.
- On the other hand, increasing span-length by 50% leads to an increase in Δ_x by an average of 22% and 18% for zero (i.e., straight bridge) and 60 degrees skew angles, respectively.
- The effect of bridge width on deck displacement cannot be predicted as it depends on almost all investigated parameters.
- As anticipated, the higher the pier, the higher the longitudinal deck displacement. However, skew angle effect on Δ_x is less significant for higher piers. For example, considering doubling the pier height leads to almost 4-times the deck displacement for straight bridges, but only 3-times the displacement for 60 degrees skew angle bridges.
- Finally, straight bridges with circular piers have greater (around 1.6 times) Δ_x values than corresponding bridges with rectangular piers. On the other hand, bridges with sharp skew angles, i.e., 60 degrees, have greater Δ_x values (around 6 times larger) relative to straight bridges for the case of rectangular piers, which means that the pier cross-section shape has the most significant influence on Δ_x values.

4. Response of Skew Bridges considering time-history analyses under seven actual ground records

4.1Selected earthquake records

As an alternative method to employ response spectrum analysis for the determination of design straining actions and deformations, international seismic provisions permit the use of actual suitable/representative earthquake records and perform time-history analysis. In such case, seismic provisions recommend choosing as design demand either the maximum values when three earthquake records are studied, or the average values when seven (or more) records are considered (AASHTO LRFD 2008 and EN 1998-2 2005). In this manuscript, time-history analyses are performed on the previously mentioned archetypical skew bridges considering seven real earthquake records. Such records are scaled to be independent of moment magnitude, and distance and to match a specific value of spectral acceleration of the code DRS. There are many techniques of scaling earthquake ground motion records in the literature (Behnamfar and Velni 2019, Markous *et al.* 2014, Mehanny 2009, and Shome and Cornell 1999 among others). Among them, the most basic and famous approach is where the peak ground acceleration, PGA, of the record is scaled to match the code value for a specific seismic zone. Another wide-spread technique that is record-structure specific, which is utilized herein, is not related to the PGA, but to the spectral acceleration at the fundamental period of the structure. As shown in Fig. 14, response spectra of the seven selected

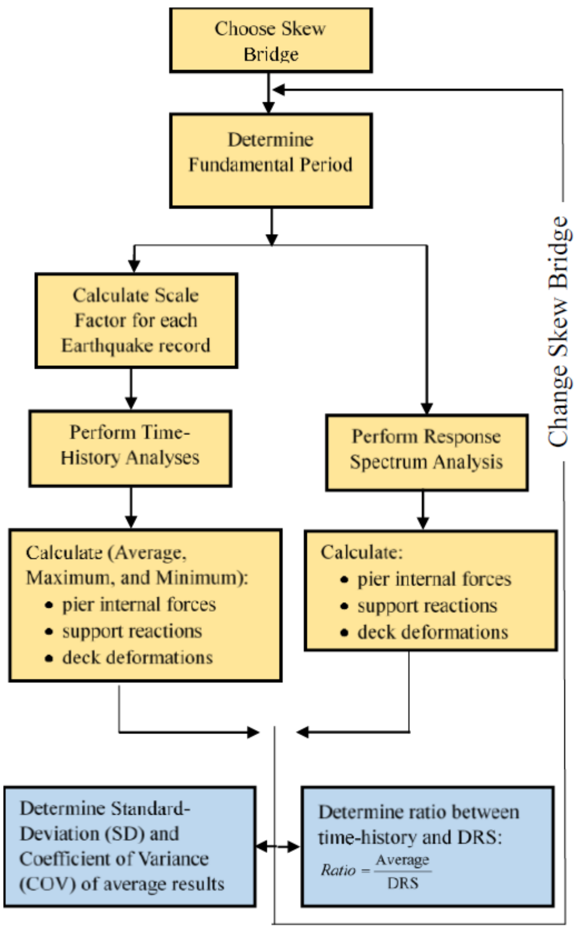

Fig. 15 Flow chart of the time history (THA) and response spectrum (RSA) comparative analyses

earthquake records are developed and scaled. All response spectra are scaled to match the spectral acceleration value retrieved from the code DRS at the fundamental period of any specific bridge under consideration. In other words, earthquake records in the present research are scaled with different scale factors that depend not only on each investigated skew bridge modal properties but also on the earthquake record itself. Fig. 14 depicts for illustration purposes sample scaled selected records for one of the skew bridges considered in the present research.

4.2 Time History (THA) versus Response Spectrum Analysis (RSA) results

In this section, the results of the time history analyses under the seven scaled actual records for the investigated skew bridges are compared-according to the steps delineated in the flow chart in Fig. 15 - to those retrieved from the response spectrum analysis under the code DRS previously presented. First, the fundamental period is determined for each studied skew bridge. Then, each of the seven real earthquake records is scaled using the previously mentioned record-structure specific scaling technique (see sample scaled records in Fig. 14), and time-history analyses are hence carried out. Subsequently, the average, maximum and minimum straining actions and deck longitudinal

Table 1 Ratios between average time-history results and corresponding response spectrum results

		Skew Angle (Degree)							Average
		0	10	20	30	40	50	60	
Base Shear (V_{22})	Longitudinal	90%	90%	93%	93%	93%	93%	93%	92%
	Transverse		78%	76%	74%	74%	65%	62%	71%
Base Shear (V_{33})	Longitudinal		91%	92%	93%	93%	93%	94%	93%
	Transverse	60%	56%	57%	58%	58%	55%	57%	58%
Pier's Torsion	Longitudinal		96%	97%	97%	97%	95%	94%	96 %
	Transverse	64%	64%	67%	71%	73%	66%	72%	68%
Abutment Bearing Reaction	Longitudinal		91%	92%	93%	93%	91%	93%	92%
	Transverse	69%	62%	63%	66%	66%	87%	74%	70 %
Deck's Deformations	Longitudinal	90%	91%	92%	94%	94%	94%	95%	93 %

displacement are determined along with some statistical measures such as the coefficient of variation (COV).

The ratios between the average straining actions and deformation determined from time history analyses under the seven scaled records for each skew bridge and the corresponding values determined from response spectrum analysis are listed in Table 1. It may be observed from the table that this ratio shows very close - and nearly identical - values for different straining actions and deck longitudinal displacement among various considered skew angles when the earthquake is assigned along the longitudinal direction of the bridge. This infers that either of the two analysis approaches (time history under scaled records and response spectrum under code DRS) may be followed interchangeably without any loss of accuracy in the results in case the user is interested in the earthquake loading in the bridge's longitudinal direction. Conversely, when applying the earthquake records in the bridge's transverse direction, noticeable differences may be observed in different reported straining actions and deck displacement among various investigated skew angles.

In addition, this ratio (THA/RSA) scoring values more than 90% for all skew angles and for various studied seismic demands in case of earthquake applied in the longitudinal direction of the bridge confirms the superiority of the scaling technique adopted herein for this specific case.

On the other hand, this ratio - averaged among various investigated skew angles - is only around 70% for pier base shear V_{22}, pier torsion and abutment transverse support reaction, and around 60 % for pier base shear V_{33}, when the earthquake is applied in the transverse direction. This implicitly shows that the adopted single-valued scaling technique is not adequate for records applied in the transverse direction of the bridge. A potential candidate for scaling records that may be more effective for the transversely applied earthquakes could be achieved through combining in a vector format the spectral acceleration values at a few adequately pre-selected periods of vibration. However, investigating more suitable scaling approaches for the transversely applied earthquake records is beyond the scope of the present research.

Finally, it is worth reporting the values of the coefficient of variation (COV) for the ratio (THA/RSA) for different

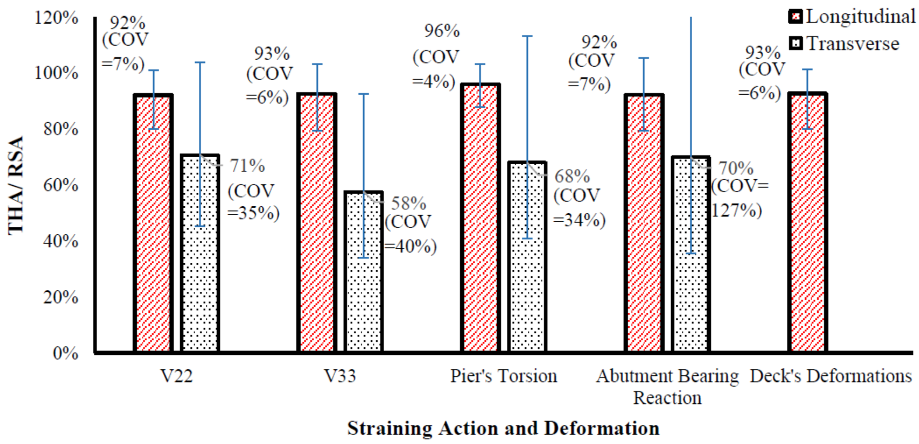

Fig. 16 Statistical results of the "time history/response spectrum" seismic design demand ratios averaged among all investigated skew bridges for both longitudinally and transversely applied earthquake records

monitored seismic design demands as shown in Fig. 16. Calculated COV values for the THA/RSA results are typically very mild (less than 10%) when averaged among all investigated skew angles in case the earthquake is applied in the longitudinal direction of the bridge. On the other hand, corresponding COV values averaged for all skew angles for the case of the earthquake applied in the transverse direction are exceptionally large (exceeding 35%) thus reflecting a large inherent dispersion in the results. Accordingly, minimum and maximum errors between averaged time-history results and corresponding response spectrum results are expected to be significantly low only in case of earthquake applied in the longitudinal direction. As such, RSA can be effectively used in determining seismic demands in terms of internal forces as well as deck longitudinal displacement only in case the earthquake is applied in the longitudinal direction of the bridge. On the other hand, THA is the suitable option if the response under transverse earthquake loading is sought.

5. Conclusions

Seismic vulnerability of bridges which constitute a major asset in the infrastructure of any country, is a critical issue that typically receives an increased attention in an effort to warrant an effective response to seismic hazards with minimal or contained damage. Unlike straight bridges, understanding the seismic response of skew bridges is a real challenge to bridge designers, researchers, authorities responsible for bridge maintenance and management, as well as seismic code developers, and is therefore worth investigating.

The current research has tackled this critical topic of the seismic response of skew bridges through developing an overwhelming bin of archetypical skew bridges that encompasses various relevant permutations of geometric design parameters (pier height, deck width, span length, number of spans, pier-to-deck connection) and abutment bearing articulations, and subsequently performing comprehensive numerical finite element investigation through conducting extensive seismic response spectrum and time history analyses. Results of the analyses have focused on modal characteristics of the various investigated skew bridge schemes, as well as on monitored seismic design demands such as shear and torsion demand in piers, bearings' transverse reactions at abutments, and deck longitudinal displacement.

Vis-à-vis modal properties, the higher the skew angle, the less the fundamental period. The average reduction in the fundamental period considering rectangular and circular pier shapes (per 10 degrees change in skew angle) is around 20% and 5%, respectively. In addition, it is found that bridges with skew angles less than 30 degrees can be treated as straight bridges for the purpose of calculating modal mass participation factors. Moreover, unlike straight bridges, it has been typically noted that skew bridges experience non-negligible torsion and bi-directional pier base shears. Skew bridges further (typically) experience non-zero values for the transverse reaction of abutment's bearings even when the earthquake is applied in the bridge longitudinal direction.

Furthermore, for skew bridges resting on rectangular piers with either monolithic or hinged pier-to-deck connections, the deck seismic longitudinal displacement is inversely proportional to the skew angle with a steep relation for small skew angles (up to 20 degrees) followed by a mild relation for larger skew angles up to the largest studied angle (namely, 60 degrees). Finally, one may claim that the response spectrum analysis can be effectively used instead of the more expensive and time-consuming time history analysis without any appreciable loss of accuracy to adequately estimate seismic design demands of skew bridges only for earthquakes applied in the longitudinal direction of the bridge. Concluding the key findings of the manuscript is intended to be concise rather than reiterating information clearly and comprehensively identified in the body of the manuscript, and to only focus on some major highlights to avoid distracting the readers from the useful aspects of the results.

The outcome of the present effort is anticipated to serve as a seminal work for practitioners and researchers in the area of seismic design of bridges as well as an inventory for code developers to better identify the key aspects of the seismic response of skew bridges in order to promote appropriate relevant effective and simplified seismic design guidelines. Similar further efforts are yet to be expected to achieve satisfactorily these goals.

References

AASHTO LRFD (2008), American Association of State Highway and Transportation Officials, Washington, D.C., USA.

Apirakvorapinit, P. (2005), "Analytical investigation of seismic damage to skewed bridges in california", Ph.D. Dissertation, Illinois Institute of Technology, Chicago, USA.

Apirakvorapinit, P., Mohammadi, J. and Shen, J. (2012), "Analytical investigation of potential seismic damage to a Skewed Bridge", *Prac. Period. Struct. Des. Constr.*, ASCE, **16**(1), 5-12. https://doi.org/10.1061/(ASCE)SC.1943-5576.0000094.

Ayoub, E., Malek, C. and Helmy, G. (2013), "Effect of skewness on bridges subjected to seismic loading", *IABSE Conference Rotterdam*, Netherlands, May.

Ayoub, E., Malek, C. and Helmy, G. (2014), "Response of three span skew bridges subjected to longitudinal and transversal earthquake loading", *37th IABSE Symposium*, Madrid, Spain, September.

Behnamfar, F. and Velni M.T. (2019), "A rapid screening method for selection and modification of ground motions for time history analysis", *Earthq. Struct.*, **16(**1), 29-39. https://doi.org/10.12989/eas.2019.16.1.029.

Chen, L. and Chen, S. (2016), "Seismic fragility performance of skewed and curved bridges in low-to-moderate seismic region", *Earthq. Struct.*, **10**(4), 789-810. https://doi.org/10.12989/eas.2016.10.4.789.

CSI, SAP2000 Integrated Software for Structural Analysis and Design, Computers and Structures Inc., Berkeley, California.

ECP 201 (2008) Egyptian Code of Practice no. 201 for Determination of Loads and Forces for the Structural and Civil Works, Research Centre for Housing and Construction, Ministry of Housing, Utilities and Urban Planning, Cairo, Egypt.

EN 1998-2 Eurocode 8 (2005) Design of Structures for Earthquake Resistance, Part 2: Bridges, Comité Européen de Normalisation, Brussels, Belgium.

Fakhry, M.F. (2019), "Investigating seismic response of skew bridges for various permutations of geometric design parameters and abutment bearings articulations", M.Sc. Thesis, Faculty of Engineering, Cairo University

Farag, M.M.N, Mehanny, S.S.F. and Bakhoum, M.M. (2015), "Establishing optimal gap size for precast beam bridges with a buffer-gap-elastomeric bearings system", *Earthq. Struct.*, **9(**1), 195-219. https://doi.org/10.12989/eas.2015.9.1.195.

Ghosh, J. and Padgett, J. E. (2012), "Impact of multiple component deterioration and exposure conditions on seismic vulnerability of concrete bridges", *Earthq. Struct.*, **3**(5), 649-673. https://doi.org/10.12989/eas.2012.3.5.649.

Kun, C., Yang, Z. and Chouw, N. (2018), "Seismic response of skewed bridges including pounding effects", *Earthq. Struct.*, **14(**5), 467-476. https://doi.org/10.12989/eas.2018.14.5.467.

Liu, Y., Paolacci, F. and Lu, D.G. (2017), "Seismic fragility of a typical bridge using extrapolated experimental damage limit states", *Earthq. Struct.*, **13(**6), 599-611. https://doi.org/10.12989/eas.2017.13.6.599.

Maleki, S. (2001), "Free vibration of skewed bridges", *J. Vib. Control*, **7**(7), 935-952. https://doi.org/10.1177/107754630100700701.

Maleki, S. (2002), "Deck modeling for seismic analysis of skewed slab- girder bridges", *Eng. Struct.*, **24**(10), 1315-1326. https://doi.org/10.1016/S0141-0296(02)00066-4.

Maleki, S. (2005), "Seismic modeling of skewed bridges with elastomeric bearings and side retainers", *J. Bridge Eng.*, ASCE, **10**(4), 442-449. https://doi.org/10.1061/(ASCE)1084-0702(2005)10:4(442).

Markous, N.A., Mehanny, S.S.F. and Bakhoum, M.M. (2014), "Scaling of earthquake ground motion records for seismic analysis and design of bridges", *J. Egypt. Soc. Eng.*, **53**(2).

Mehanny, S.S.F. (2009), "A broad-range power-law form scalar-based seismic intensity measure", *Eng. Struct.*, **31**(7), 1354-1368. https://doi.org/10.1016/j.engstruct.2009.02.003.

Meng, J.., and Lui, E. (2000), "Seismic analysis and assessment of a skew highway bridge", *Eng. Struct.*, **22**(11), 1433-1452. https://doi.org/10.1016/S0141-0296(99)00097-8.

Ramanathan, K., Jeon, J.S., Zakeri, B., DesRoches, R. and Padgett, J.E. (2015), "Seismic response prediction and modeling considerations for curved and skewed concrete box-girder bridges", *Earthq. Struct.*, **9**(6), 1153-1179. https://doi.org/10.12989/eas.2015.9.6.1153.

Shome, N. and Cornell, C.A. (1999), "Probabilistic seismic demand analysis of nonlinear structures", Rep. No. RMS-35, Reliability of Marine Structures, Dept. of Civil and Eng., Stanford University, March.

Wakefield, R., Nazmy, A. and Billington, D. (1991), "Analysis of seismic failure in skew RC bridge", *J. Struct. Eng.*, ASCE, **117**(3), 972-986. https://doi.org/10.1061/(ASCE)0733-9445(1991)117:3(972).

Whelan, M. and Janoyan, K. (2012), "Assessment of simplified linear dynamic analysis of a multispan Skew Bridge on steel-reinforced elastomeric bearings", *J. Bridge Eng.*, ASCE, **16**(1), 151-160. https://doi.org/10.1061/(ASCE)BE.1943-5592.0000218.

CC

Notations

The following symbols are used in this paper

W	Bridge width (in m)
L	Bridge span measured center to center of piers (in m)
H	Pier height (in m)
β	Skew angle (in degrees)
E	Young's modulus (in MPa)
ν	Poison's ratio
T_1	First (fundamental) period of the bridge (in s)
T_2	Second period of the bridge (in s)
M_{ux}	Longitudinal mass participation factor (percentage)
M_{uy}	Transversal mass participation factor (percentage)
V_{22}	Pier base shear along an axis with a clockwise angle β measured from the bridge longitudinal axis - weak-axis shear for case of rectangular piers (in kN)
V_{33}	Pier base shear along an axis with an anti-clockwise angle 90º-β measured from the bridge longitudinal axis - strong-axis shear for case of rectangular piers (in kN)
R_a	Transverse abutment bearing reaction ratio when earthquake is in bridge longitudinal direction (%)
R_b	Transverse abutment bearing reaction ratio when earthquake is in bridge transverse direction (%)
Δ_x	Longitudinal deck's displacement (in mm)